THE TRANSIENT GRATING AS A PROBE FOR POLARITON DYNAMICS

Knoester, Jasper

Published in:
Journal of Luminescence

DOI:
10.1016/0022-2313(91)90095-D

Publication date:
1991

Journal of Luminescence 48 & 49 (1991) 152–156
North-Holland

The transient grating as a probe for polariton dynamics

Jasper Knoester

Department of Physical Chemistry, University of Groningen, Nijenborgh 16, 9747 AG Groningen, The Netherlands

A theory is presented that microscopically accounts for the role of polariton propagation in the transient grating experiment. The basis of our theory is formed by coupled equations of motion for polariton amplitudes and coherences, in which we account for polariton–phonon scattering. It is demonstrated that at low temperature the transient grating experiment probes polariton dynamics. Explicit results for the transient grating signal are obtained within two specific (strong-collision) models for polariton scattering.

1. Introduction

The effect of retarded interactions on the nonlinear optical response of condensed phases has recently attracted much attention [1–4]. As these interactions are mediated by the transverse electric field, they can be accounted for by considering the combined eigenmodes of the microscopic radiation field and the material Coulomb excitons (which only include the instantaneous interactions). These eigenmodes are the (excitonic) polaritons, and retardation effects are also called polariton effects. If retarded interactions are neglected, the optical response of a sample is determined by the response of the excitons to the external electric fields [5]. The optical resonances then occur at (differences or sums of) *exciton* frequencies; line broadening is determined by scattering rates of excitons, etc. This picture is in general valid if the exciton–radiation field coupling (characterized by f, where f^2 is proportional to the oscillator strength per unit volume, see section 3) is much smaller than the coupling of the excitons to other degrees of freedom, such as phonons, lattice defects, etc. (characterized by an exciton damping rate Γ_{ex}) [2,3]. If $f \ll \Gamma_{ex}$, namely, the exciton has no time to couple coherently to the photons before it is damped and the maximum mixture between excitons and photons in their combined eigenmodes is of the order f/Γ_{ex}. On the other hand, if $f \gg \Gamma_{ex}$, the unperturbed eigenmodes in the system are strongly mixed combinations of excitons and photons, and in an optical experiment one must expect to probe polariton properties. The condition $f \gg \Gamma_{ex}$ is typically met in low temperature pure crystals and at a sufficiently high density of oscillator strength.

One of the recent studies that stimulated the discussion of polariton effects in nonlinear optics, is a series of transient grating (TG) experiments in low temperature anthracene crystals performed by Rose et al. [6]. TGs are traditionally viewed as ideal probes for exciton migration [6–8]. Agranovich et al. [1], however, noted that the diffusion constant reported in ref. [6] was too high for excitons and they suggested that the experiments should be interpreted in terms of polariton diffusion. The rationale behind this is that the polariton group velocity is in general much higher than that of undressed excitons. Although, the role of polaritons is generally accepted nowadays, a microscopic theory treating the creation, evolution, and detection of the TG in terms of polaritons is still lacking. In this paper we present such a theory, based on equations of motion for polariton variables.

2. Equations of motion

We will consider a standard TG experiment carried out on a molecular crystal. For simplicity,

we assume the lattice to contain one two-level molecule per unit cell (transition frequency Ω and transition dipole $\boldsymbol{\mu}$). We work within second quantization. As is well-known, it is possible to transform from the exciton $(\hat{B}_k^\dagger, \hat{B}_k)$ and photon $(\hat{a}_k^\dagger, \hat{a}_k)$ creation and annihilation operators at wave vector $\boldsymbol{k}$ to a set of polariton creation and annihilation operators $(\hat{\xi}_{k\nu}^\dagger, \hat{\xi}_{k\nu})$ that diagonalize the total Hamiltonian in the Bose approximation (see, e.g., ref. [3]). This yields the familiar two-branch polariton dispersion diagram (fig. 1). Going beyond the Bose approximation, the full equation of motion for the polariton annihilation operator at wave vector $\boldsymbol{k}$ in branch ν reads (all operators taken at time t) [9]:

$$\frac{\mathrm{d}}{\mathrm{d}t}\hat{\xi}_{k\nu} = -\mathrm{i}\omega_{k\nu}\hat{\xi}_{k\nu} + \tfrac{1}{2}\sum_{k',\nu'}[\gamma\hat{\xi}_{k'\nu'} - \gamma^*\hat{\xi}_{k'\nu'}^\dagger, \hat{W}(k-k')]_+, \quad (1)$$

where the k'-sum (as all other wave vector sums in this paper) extends over the first Brillouin zone only, $[\hat{A}, \hat{B}]_+ \equiv \hat{A}\hat{B} + \hat{B}\hat{A}$, and γ is a c-number which depends on k, k', ν, and ν'; the exact form of γ is not important here (* denotes complex conjugation). Finally, $\hat{W}(k)$ is the exciton population operator at wave vector k. For harmonic oscillators (bosons) this operator vanishes identically and the last term in eq. (1) is absent. For excitons in a crystal of two-level molecules, however, we have

$$\hat{W}(k-k') = \frac{2}{N}\sum_{k''}\hat{B}_{k'+k''}^\dagger\hat{B}_{k+k''} \approx \frac{2}{N}\sum_{k''\nu\nu'}x_{k'+k''\nu'}x_{k+k''\nu}^*\hat{\xi}_{k'+k''\nu'}^\dagger\hat{\xi}_{k+k''\nu} \quad (2)$$

(N is the number of molecules), and neglecting this operator is referred to as the Bose approximation, which linearizes eq. (1). The population operator allows for nonlinear effects in the polariton evolution. The last step in eq. (2) involves the inverse polariton transformation [3], where $x_{k\nu}$ is the transformation coefficient relating $\hat{\xi}_{k\nu}$ to $\hat{B}_k$; the coefficient between $\hat{\xi}_{k\nu}$ and $\hat{B}_k^\dagger$ is usually very small [3] and has been neglected above. We note that eq. (2) has been derived from the multipolar Hamiltonian, using the equations of motion developed in ref. [5]. A theory based on the minimal coupling Hamiltonian will give similar equations.

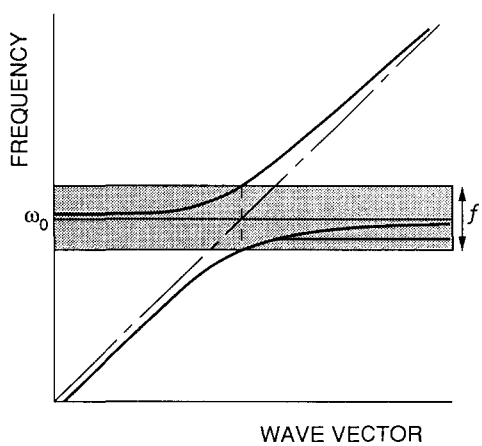

Fig. 1. Typical polariton dispersion diagram (thick solid curves). The diagonal line represents photons ($\omega = kc$); the horizontal line (ω_0) denotes the excitons, where dispersion has been neglected. The polaritons within the shaded region take part in the first scattering model discussed in section 3. f is a measure for the density of oscillator strength and is defined in the text. The polariton stop gap is not shown.

In terms of polaritons, the TG experiment is formulated as follows. At time $t = 0$, two crossed pump pulses (wave vectors k_i' $[i = 1, 2]$) are incident on the crystal and create polaritons with wave vectors k_i, branches ν_i, and amplitudes $\langle\hat{\xi}_{k_i\nu_i}\rangle$ ($\langle\cdots\rangle$ denoting the expectation value) determined by matching the boundary conditions for their electromagnetic field components to the external laser fields. These polaritons form a grating in the crystal, which is probed after time τ by applying a third laser pulse (k_3'). This pulse creates polaritons at (k_3, ν_3), which scatter on the grating, resulting in signal polaritons with $k_s = k_1 - k_2 + k_3$. Finally, these signal polaritons cause the detected electric field outside the crystal with wave vector $k_1' - k_2' + k_3'$ and intensity $I(t) \propto |\langle\hat{\xi}_{k_s\nu_s}(t)\rangle|^2$.

To evaluate the amplitude $\langle\hat{\xi}_{k_s\nu_s}(t)\rangle$, we take the expectation value of eq. (1), which on its right-hand side involves expectation values of products of operators. In order to truncate the thus generated hierarchy of successively more involved products of operators, we factor the nonlinear term and

obtain:

$$\frac{\mathrm{d}}{\mathrm{d}t}\langle\hat{\xi}_{\boldsymbol{k}_s\nu_s}(t)\rangle = -[\mathrm{i}\omega_{\boldsymbol{k}_s\nu_s} + \Gamma(\boldsymbol{k}_s, \nu_s)]\langle\hat{\xi}_{\boldsymbol{k}_s\nu_s}(t)\rangle + \gamma\langle\hat{\xi}_{\boldsymbol{k}_3\nu_3}(t)\rangle\langle\hat{W}(\boldsymbol{k}_1-\boldsymbol{k}_2, t)\rangle. \quad (3)$$

Here, $\Gamma(\boldsymbol{k}_s, \nu_s)$ represents the exciton damping due to phonon scattering, which can be obtained from the standard exciton–phonon interaction [3]. Mixing of the polariton branches due to this scattering is neglected. If we assume that the probe pulse amplitude relaxes fast on the time scale of the grating decay (off-resonance detection), we find for the time-integrated signal intensity:

$$S(\tau) \propto |\langle\hat{W}(\boldsymbol{k}_1-\boldsymbol{k}_2, \tau)\rangle|^2. \quad (4)$$

The TG signal is thus determined by the exciton population at the grating wave vector $\boldsymbol{k}_1-\boldsymbol{k}_2$. The same result is obtained in the traditional (exciton) theories for the TG [7,8]. The new element in our approach, however, is that during the pump-probe delay the evolution of the population is governed by polariton propagation rather than exciton propagation. From eqs. (2) and (3) it is seen that during this period the relevant variables are polariton coherences, which obey:

$$\frac{\mathrm{d}}{\mathrm{d}t}\langle\hat{\xi}^\dagger_{k\nu}(t)\hat{\xi}_{k'\nu'}(t)\rangle = \mathrm{i}[\omega_{k\nu}-\omega_{k'\nu'}]\langle\hat{\xi}^\dagger_{k\nu}(t)\hat{\xi}_{k'\nu'}(t)\rangle - \sum_{k''\nu''\nu'''}\Gamma(\boldsymbol{k}, \boldsymbol{k}', \boldsymbol{k}'', \boldsymbol{\nu})\langle\hat{\xi}^\dagger_{k+k''\nu''}(t)\hat{\xi}_{k'+k''\nu'''}(t)\rangle, \quad (5)$$

where $\boldsymbol{\nu}$ stands for $(\nu, \nu', \nu'', \nu''')$. This equation follows from eq. (1) and its Hermitian conjugate. Notice that now the nonlinear term is neglected, as it would eventually lead to an intensity of higher than third order in the laser field intensities. The last term in eq. (5) results from polariton–phonon scattering and can be derived from first principles using the projection technique applied in ref. [3]. It is important that the thermal average over the phonon bath involved in this technique, automatically restricts the scattering to couple the coherence at $(\boldsymbol{k}, \boldsymbol{k}')$ only to coherences at $(\boldsymbol{k}+\boldsymbol{k}'', \boldsymbol{k}'+\boldsymbol{k}'')$, i.e. the difference of wave vectors within the coherence is maintained. Equation (5) is the heart of the TG experiment. A similar equation governs the exciton theory of the TG, but then $\omega_{k\nu}$ is replaced by the exciton dispersion relation and the scattering kernel describes scattering of excitons [7–9]. It is on this level that it becomes clear that the TG probes *polariton* motion. Although the scattering kernel $\Gamma(\boldsymbol{k}, \boldsymbol{k}', \boldsymbol{k}'', \boldsymbol{\nu})$ can in principle be calculated in detail [9], it must in practice be modeled to obtain explicit results. The initial condition to eq. (5) can be obtained by factoring the polariton coherences $\langle\hat{\xi}^\dagger_{k\nu}(0)\hat{\xi}_{k'\nu'}(0)\rangle$ right after the pump pulses into products of the polariton amplitudes $\langle\hat{\xi}^\dagger_{k\nu}(0)\rangle \times \langle\hat{\xi}_{k'\nu'}(0)\rangle$, which are proportional to the amplitudes of the external laser fields. This factorization is allowed, because scattering has not yet established correlations between the polaritons at those early times. A general result which follows from eq. (5), is that in absence of scattering the TG signal $S(\tau)$ will not decay (the system is then prepared in an eigenstate).

3. Scattering models

In this section, we discuss two specific models for the scattering kernel Γ which allow for analytical solution of the signal. The first model is similar to the Haken–Strobl model for exciton dephasing, in which $\Gamma(\boldsymbol{k}, \boldsymbol{k}', \boldsymbol{k}'') = \Gamma\delta_{\boldsymbol{k}'',\boldsymbol{0}} - \Gamma/N$: all excitons are scattered into each other with equal rates [7–9]. This model is a high temperature strong collision model, which is analytically solvable. Employing the same model for polaritons is naive, because these excitations span an enormous bandwidth. Furthermore, we must realize that only the exciton component of the polariton is coupled to the phonon bath. A simple model which includes this idea assumes that all exciton-like polaritons are scattered into each other with equal rates. Here, exciton-like refers to those polaritons with $|x_{k\nu}|^2 \geq \frac{1}{2}$; these polaritons form the upper branch for $|\boldsymbol{k}|c < \omega_0$ and the lower branch for $|\boldsymbol{k}|c > \omega_0$, with ω_0 ($\approx\Omega$) the exciton frequency at optical wave vectors (fig. 1). We thus consider only one polariton at each wave vector. For this model, eq. (5) can be solved using a T-matrix analysis. In the limit of large scattering rate Γ, the thus obtained TG signal

is characteristic of diffusive polariton motion [9]:

$$S(\tau) = S(0)\exp[-2|\boldsymbol{k}_1 - \boldsymbol{k}_2|^2 v_p^2 \tau/3\Gamma], \quad (6)$$

where v_p is the effective polariton group velocity, defined by an integral over the polariton dispersion curve. For dipolar dispersionless excitons, we estimate:

$$(v_p/c)^2 = \pi \frac{f}{\Omega}\left(\frac{a}{\lambda_0}\right)^3, \quad (7)$$

with a the lattice constant and λ_0 the vacuum wavelength corresponding to the transition frequency Ω; c is the vacuum velocity of light. The parameter f is a measure of the oscillator strength per unit volume and is defined through $f^2 \equiv 8\pi\rho\Omega\mu^2/\hbar$, with ρ the molecular number density. f has the dimension of a frequency and equals the separation between the upper and lower polariton branch at the wave vector ω_0/c, where the exciton and photon dispersion curves cross (fig. 1). Equation (7) yields estimates of $v_p \approx 10^6$ cm/s and $v_p \approx 10^5$ cm/s for anthracene and naphthalene, respectively.

The second model that we discuss here is inspired on the explanation by Agranovich et al. [1] for the anthracene TG experiments mentioned in the introduction. We assume that the pump pulses have frequencies just in the exciton band, so that they excite high wave vector polaritons with a very strong exciton character. The initially created polariton coherences $\langle \hat{\xi}^\dagger_{k\nu}\hat{\xi}_{k'\nu'}\rangle$ will now relax rapidly until $(\boldsymbol{k}+\boldsymbol{k}')/2$ reaches the polariton bottleneck region, creating a new effective initial condition for the grating (fig. 2) [9]. It is crucial that this relaxation occurs through a scattering kernel like the one in eq. (5), so that after the relaxation the grating wave vector $\boldsymbol{k}'-\boldsymbol{k} = \boldsymbol{k}_1 - \boldsymbol{k}_2$ is still "memorized". We now assume that the polaritons within the bottleneck region scatter into each other with equal rates (say Γ). This again defines a solvable strong collision model for a restricted set of polaritons. Let the polariton group velocity within the bottleneck be denoted v_b. Then in the limit of strong scattering ($\Gamma \gg |\boldsymbol{k}_1 - \boldsymbol{k}_2| v_b$), the motion is diffusive on the length scale of the experiment and we recover eq. (6) with v_p replaced by v_b. In the opposite limit ($\Gamma \ll |\boldsymbol{k}_1 - \boldsymbol{k}_2| v_b$), the signal will decay according to S(0) exp($-2\Gamma\tau$).

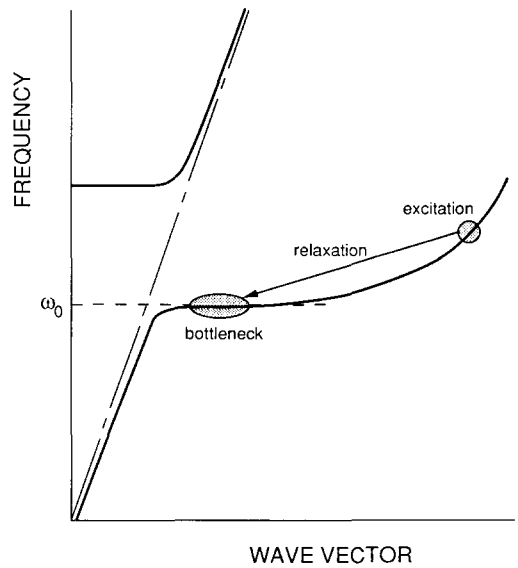

Fig. 2. Illustration of the second polariton scattering model discussed in section 3. Compared to fig. 1, a larger part of the Brillouin zone is shown and a finite effective exciton mass is included. Polaritons are excited by pulses just above ω_0 (the $\boldsymbol{k} = \boldsymbol{0}$-exciton frequency) and relax fast to the bottleneck, where the actual TG decay takes place.

4. Discussion

In this paper we presented a microscopic theory for the TG experiment that accounts for the role of polariton propagation. The present theory is a demonstration of the polariton hierarchy proposed in ref. [5], which may equally well be applied to other experiments. Within our description, the TG signal is determined by the exciton population. This result is also obtained from the traditional theories for the TG, which consider excitons interacting with external electric fields, and may be understood from the fact that the population is the only nonlinearity in a system of two-level molecules. The crucial difference with the exciton theories is that during the pump-probe delay the evolution of the system is determined by propagation of polaritons instead of excitons. Even though there are no external electric fields during this period, the internal (microscopic) electric field cannot be switched off and the dynamics of the coupled exciton-photon system must determine

the outcome of the TG experiment. The TG thus probes polariton propagation and in particular depends strongly on polariton-phonon scattering. Two analytically solvable strong collision scattering models were discussed. Our equations-of-motion approach is, however, ideally suited to incorporate more general and elaborate scattering kernels. In doing so, one may be led by intuition and specific knowledge about the system that is considered. Equation (5) for the polariton coherences is in essence a transport equation and for certain types of scattering kernels, a connection to the theory of Boltzmann equations can readily be made [9]. In general, polaritons must be expected to cause a faster TG decay than excitons. A nice demonstration of that is our result, eq. (7), which was derived in an infinite effective exciton mass approximation. Within this approximation, the exciton theory for the TG signal predicts no decay at all [7,8] whereas the polariton result shows fast diffusive decay. We finally note that the derivation of eq. (7) is based on the assumption that polariton effects are strong ($f \gg \Gamma_{ex}$; see introduction). In the opposite limit, the polaritons automatically decouple into photons and damped excitons, and the usual exciton theory is recovered.

Acknowledgements

It is a pleasure to thank Professor S. Mukamel for many stimulating discussions. This work is supported by the Netherlands Organization for Scientific Research (NWO).

References

[1] V.M. Agranovich, A.M. Ratner and M. Salieva, Solid State Commun. 63 (1987) 329.
[2] S.H. Stevenson, M.A. Connoly and G.J. Small, Chem. Phys. 128 (1988) 157.
[3] J. Knoester and S. Mukamel, J. Chem. Phys. 91 (1989) 989.
[4] E. Hanamura, Phys. Rev. B 39 (1989) 1152.
[5] J. Knoester and S. Mukamel, Phys. Rev. A 41 (1990) 3812.
[6] T.S. Rose, R. Righini and M.D. Fayer, Chem. Phys. Lett. 106 (1984) 13.
[7] D.K. Garrity and J.L. Skinner, J. Chem. Phys. 82 (1985) 260.
[8] R.F. Loring and S. Mukamel, J. Chem. Phys. 83 (1985) 4353; 84 (1986) 1228.
[9] J. Knoester and S. Mukamel, Phys. Rep., in preparation.